HYDROGEN EMBRITTLEMENT IN HEAT AFFECTED ZONE OF A WELDED SHEET OF PRECIPITATION HARDENING MARTENSITIC STAINLESS STEEL

Authors: ***S. SAKHAWAT *[A], A. FALAHATI[A], K. SPIRADEK[B], H. P. DEGISCHER[A]***
Workplace: ***[a] Vienna University of Technology, Vienna Austria***
[b] Austrian ResearchCenters, Seibersdorf, Austria
**** Corresponding author. Workplace Address Institute of Materials Science and Technology***
Favoritenstrasse 9-11/E308, A-1040 Vienna
Address: ***Email: shahroz.sakhawat@tuwien.ac.at***

Abstract:

Precipitation-hardened stainless steels offer high strength, relatively good ductility, and excellent corrosion resistance. The precipitation hardening material type DIN 1.4542 is a martensitic stainless steel containing approximately 3.3 wt. % Cu and is strengthened by the precipitation of copper in the martensite matrix. Hydrogen assisted cracks generated in the heat-affected zone (HAZ) of solution treated and welded samples have been investigated.

Metallography, hardness measurements (HV), radiography, electron back scattering diffraction technique (EBSD), transmission electron microscopy (TEM) and fractography methods are used to characterize HAZ of a tungsten inert gas (TIG) weldment of thin sheets. The heat input produced precipitates in a narrow region of the HAZ. In the same region cracks are observed, the origin of which appears to be hydrogen embrittlement. Hydrogen loading tests are performed to quantify the susceptibility of material to hydrogen embrittlement.

INTRODUCTION

Precipitation hardened martensitic stainless steel is widely used in various industries due to its favorable combination of excellent mechanical properties, easy machinability, good weldability and good corrosion resistance. Material under discussion is DIN 1.4542, which is a type of 17-4 PH martensitic stainless steel, containing approximately 3,3% Cu [1-3]. It has very low carbon content and Cu is added to achieve significant strength by precipitation of Cu rich phases during tempering.

The microstructure of this steel in solution-annealed condition comprises largely precipitation free martensite containing a minor fraction of elongated δ-ferrite. The martensite phase consists of lath structure with very high density of dislocations [3]. Atom probe analysis of the solution annealed martensite phase has shown that the martensite is in a supersaturated solid solution containing all solute atoms homogeneously distributed [1]. On ageing, precipitation of coherent copper-rich clusters occur increasing hardness notably. On overaging, these coherent precipitates transform into incoherent fcc epcilon-phase precipitates [1, 4] and hardness decreases gradually [3].

One of the chief drawbacks of this material is its susceptibility to stress corrosion cracking and hydrogen embrittlement [5]. The resistance of the alloy to hydrogen embrittlement is primarily affected by the microstructure and the provision of hydrogen. Additionally, the transport of hydrogen i.e. protons in alloys depends not only on the hydrogen concentration gradient but also on the concentration of defects producing internal tensile stresses. Increasing the stress concentration makes hydrogen more aggressive as an embrittling agent. The

present study aimed at characterizing the HAZ of DIN 1.4542 and to correlate the susceptibility of hydrogen embrittlement in the HAZ to its microstructure.

2- MATERIAL AND EXPERIMENTAL METHODS

Two pieces of stainless steel sheet type DIN 1.4542 in solution annealed (SA) condition with a thickness of 1.6 mm were welded together. The chemical composition of the material is given in table 1. Welding was done by TIG without filler material with two welding passes from both sides; a macrograph of the cross-section of welded plate is shown in Fig. 1. After welding, the welded sheets were exposed to hydrogen loading during galvanic Cr plating. Some cracks perpendicular to the seam weld were noticed. Dye penetration check and radiography (Fig. 2) were carried out on the samples. Dye penetration testing shows that one side of the plate has more open cracks to the surface than the opposite side. A macrograph of one crack is shown in Fig. 3.

Table 1 Chemical composition of the material

Elements	C	Si	Mn	P	S	Ni	Cr	Cu	Nb	Fe
Composition (Wt%)	0.03	0.48	0.7	0.025	0.001	4.9	15.0	3.08	0.25	Balance

X-ray micro radiography has been performed by using a phoenix 225s microfocus tube at 120 kV and 100 μA and a PerkinElmer RID 1640 flat panel detector with 1024×1024 pixel averaging over 200 frames of 400 ms recording time. A resolution down to $(10\ \mu m)^2$/pixel has been chosen for imaging the weld-seam and the crack region. Micro radiography shows that all the cracks with different lengths begin periodically along the weld seam.
Metallography was carried out on the base metal (Fig. 4 and 5) and the welded area (Fig. 6 to 8, 10 and 11) to characterize their microstructure. Two different types of etchants were used, W II and Beraha I [6] to check delta ferrite. Micro hardness profiles across the weld, in the HAZ and base material (ST-section) were measured according to EN 6507 in Vickers HV 1 (and are presented in Fig.13.)

The SEM-EBSD technique was used for grain size mapping of HAZ (Fig. 9). The sample was first mechanically ground and polished down to 1μm diamond paste. In order to obtain EBSD patterns of good quality, it was important to remove the residual deformation in the surface layer of the specimens. Subsequently, electro-polishing was carried out on the flat surfaces in a solution of 20% perchloric acid ($HClO_4$), 70% ethanol (C_2H_5OH) and 10% ethylene glycol monobutyl ether ($CH_3(CH_2)_3OCH_2CH_2OH$) in volume at 20 °C, with the voltage of 28V for 10 s.

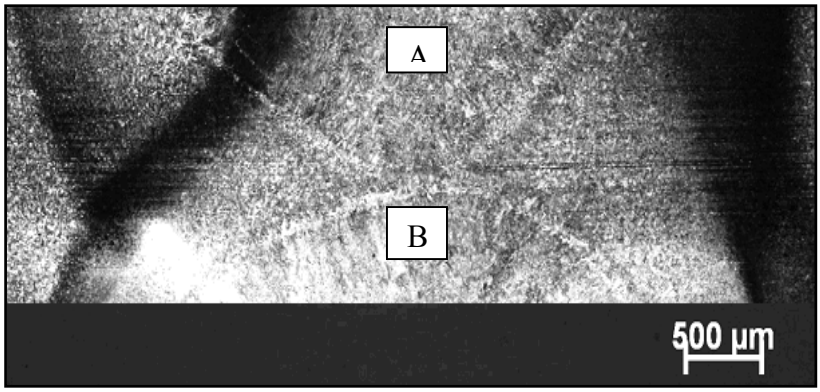

Figure 1 *Macrograph of the cross-section of welded region / Dark tinted region is visible on both sides of weld seam/ A is 1st weld pass seam: B is 2nd weld pass seam. Etchant: W II (Wallner)*

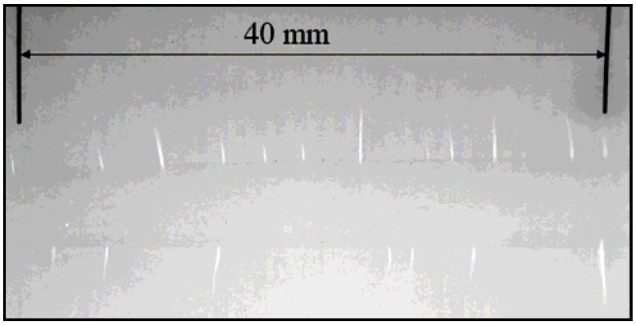

Figure 2 *X-ray micro radiography image of the welded sheet, cracks are visible on the both sides perpendicular to weld-seam (white)*

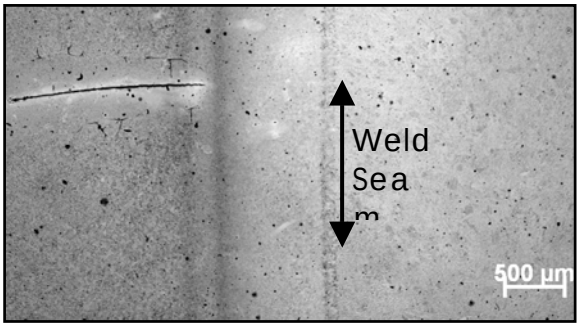

Figure 3 *Macrograph of one of the cracks/ viewed from LT direction/ Etchant: W II (Wallner)*

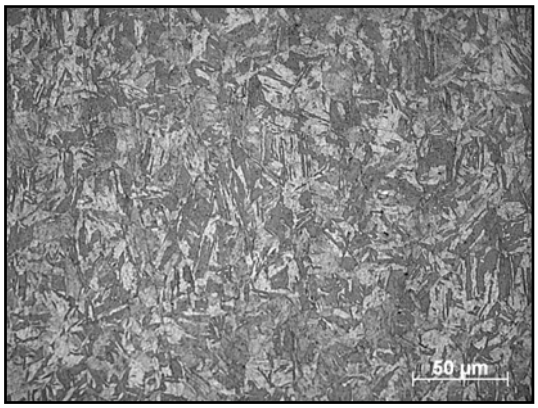

Figure 4 *Base metal with typical martensitic microstructure. No delta ferrite is visible in this micrograph (LT plane) etched with Beraha 1*

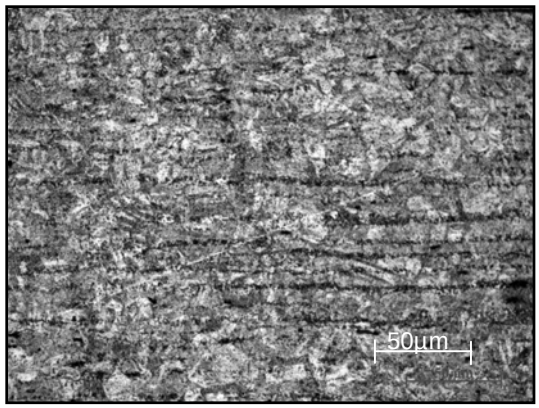

Figure 5 *Base metal etched with W II (Wallner), segregation lines are visible (ST Plane)*

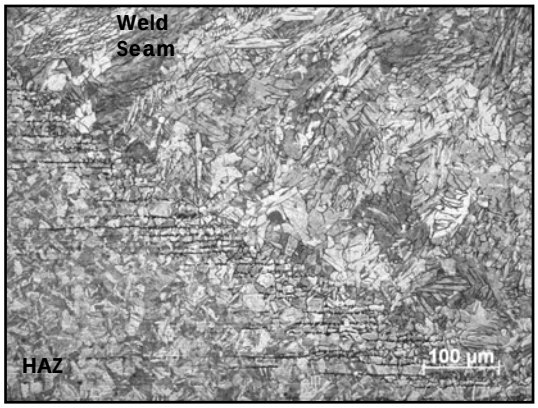

Figure 6 *Grain structure in the HAZ close to the weld seam (ST Plane).*

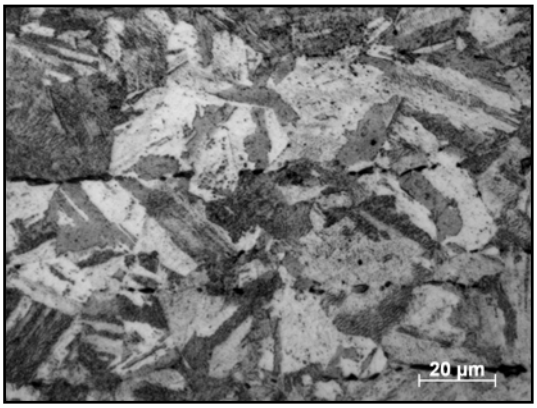

Figure 7 *Coarse grained HAZ, adjacent to fusion zone (ST Plane).*

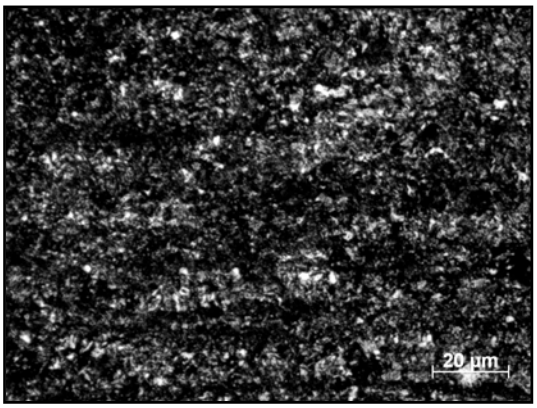

Figure 8 *Microstructure of black tinted region in the HAZ (ST Plane)*

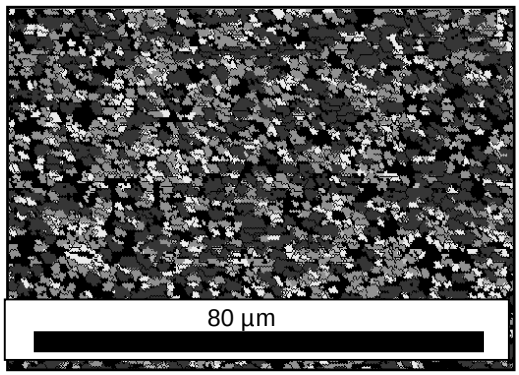

Figure 9 *Grain size mapping of region in Figure 8, by EBSD. (ST Plane). Gray scale indicates the size class*

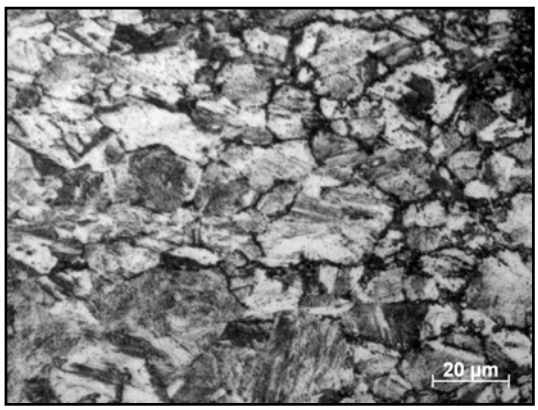

Figure 10 *Microstructure region in the HAZ adjacent to Fig. 8, (ST Plane)*

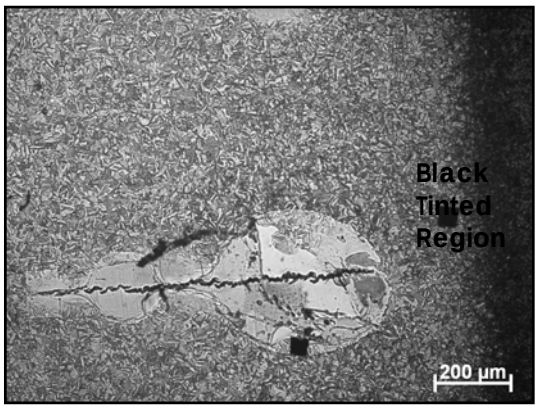

Figure 11 *Macrograph of crack, in the region shown in Figure 10. (LT Plane)*

Approximately 2 cracks per centimeter were identified with the help of radiography. Some were opened by tensile testing perpendicular to the direction of the cracks at room temperatures. The fracture surfaces were studied with scanning electron microscopy to locate and identify the crack shape (Fig. 14) and the fracture mode (Fig. 14a and 14b). Location and position of the susceptible microstructure were identified and samples prepared thereof investigated by targeted high-resolution transmission electron microscopy (HRTEM) (Fig 15 to 17).

Hydrogen-loading tests were done on base metal (in as-received condition with no aging treatment), to study the susceptibility of this material to hydrogen embrittlement under pre-stressed conditions. U-shaped bent specimens were prepared from the steel strips of size 100 x 10 x 1,6 mm^3. Initially the strips were permanent bent to the angle of 35° (Fig. 12a). Then bending angle was reduced to 20° by screwing, to pre-stress the outer side, (Fig. 12b). Before immersing into the electrolyte the samples were rinsed with distilled water and cleaned ultrasonically with acetone and were quickly dried with warm air.

During these tests, the cathodic (U shaped specimen), or hydrogen entry side, of the cell was galavanostatically polarized at a constant current density (10 mA/cm²) in 0.1 N NaOH. The anodic side, or hydrogen exit side, of the cell was held at a constant potential of 250 mV (SCE). The cell assembly was immersed in a constant temperature bath maintained at 25±1°C (Fig. 12c) [5]. Samples were taken out after every 30 minutes exposure to inspect visually if any crack appears. Samples cracked in the middle from the outer side, which was under tension after a minimum exposure of three hours in the above-mentioned conditions.

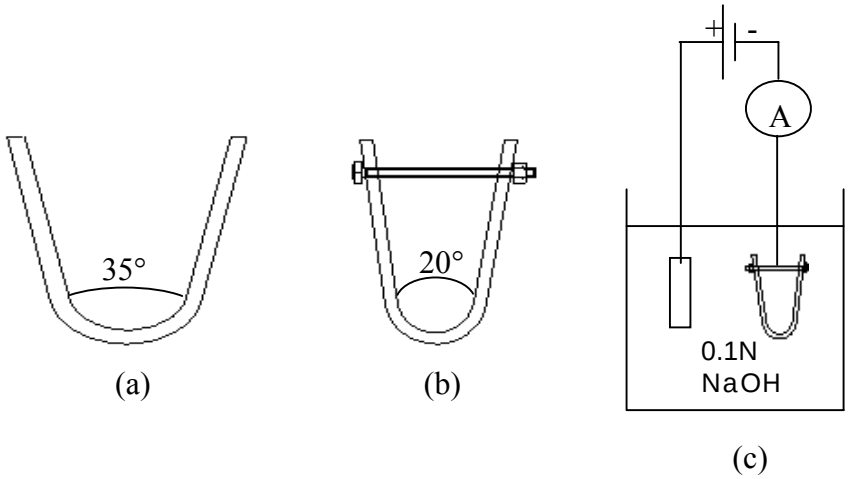

Figure 12 *Sketch of U shaped specimen used for hydrogen loading, a) Before screwing, b) After screwing to maintain tensile stress on the outer side of the bend, c) Schematic presentation of experimental setup*

RESULTS AND DISCUSSIONS

The microstructure of the unaffected as-received base metal is shown in optical micrograph (Fig. 4). As can be seen the base metal is a typical martensitic microstructure and no delta ferrite is visible in the micrograph. The average grain size of the base metal in LT direction was measured to be about 25 μm. Segregation lines are visible in ST plane in Fig. 5. Fig. 1 shows the macrostructure of cross section of the weldment showing the different regions developed. The first weld-pass is on the top and the second pass from the bottom. The weld zone has a cast microstructure, characteristic of solidification at rapid cooling yielding martensitic structure. Fig. 6 shows the cast structure of the weld seam (right), coarse-grain structure of about 50 μm size adjacent to the fusion boundary (in the middle) and a fine-grained structure. Although the duration of heating is very short, the martensite in coarse-grain region will transform into austenite and part of the reformed austenite subsequently transform into laths martensite during cooling (partially, could remain as retained austenite too [4]). Because the austenitising temperatures experienced in this narrow region during welding is generally higher than the SA temperature used, grain growth produces coarse-grained structure (Fig.7). Adjacent to the coarse grains is a fine-grained structure region of about 70 μm width. The HAZ region just next to the fine grained has a grain size similar to that of the base material. As can be seen in Fig. 1 there are also some black tinted regions on both side of the weld in the macrograph [7], which is shown in detail in Fig. 7 depicting a strongly etched sample. EBSD grain size mapping performed on this black tinted region show very fine microstructure of size 1-4 μm (Fig. 9) and the cracks, which are observed on the surface, are limited by this black tinted region (Fig. 2, 3 and 11). The microstructure is martensite with some horizontal segregation lines. Fig. 13 shows the micro hardness profile across the weld. As can be seen the peak hardness is about 0.25 mm outside the black tinted

region, which implies that full width of the HAZ is not visible and recognizable by optical micrographs.

HAZ consists of retransformed martensite (and reformed austenite [8]), overaged martensite und underaged martensite. Before welding the sheets together, they were super saturated with Cu. During continuous cooling of the welded sheets in air, some regions of HAZ have passed through temperatures, which are suitable to age these regions locally and as a result to precipitate Cu. Regarding precipitation hardening, the region close to the fusion line (retransformed martensite) could be in SA condition, after which overaging might occur further away from the fusion line to the region of peak hardness and thereafter, underaged region, to the region where the base-material hardness is reached (about 1mm after max. hardness peak).

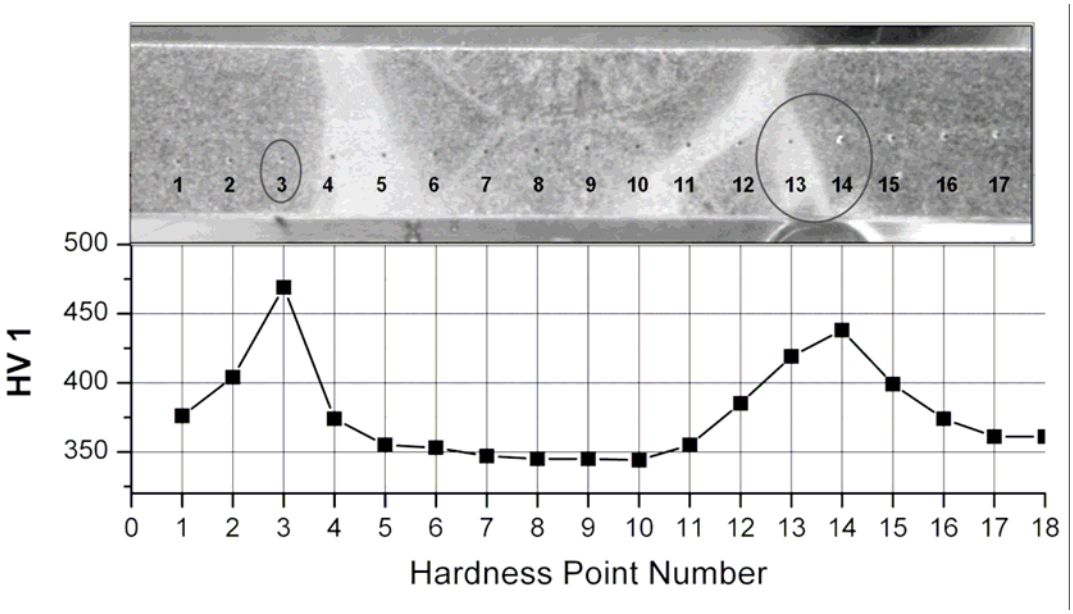

Figure 13 *Micro hardness measurements along cross-section of the weld and the HAZ*

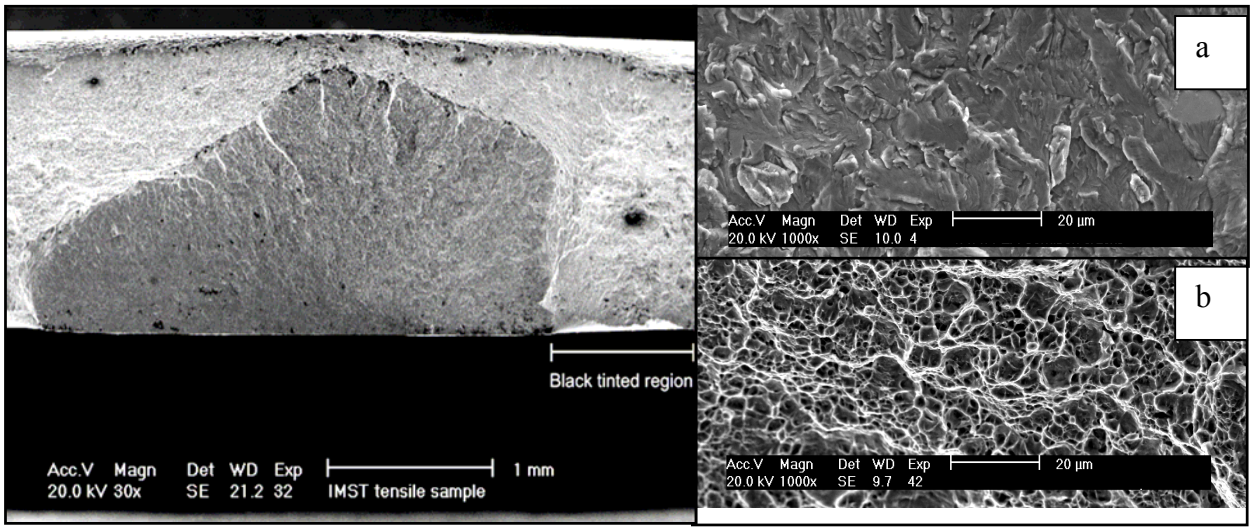

Figure 14 *Crack fractography, white crack propagation lines pointing towards crack initiation, a): Cracked surface showing brittle fracture which has propagated trans-granularly characterizing hydrogen embrittlement b) Portion of the enforced fracture surface of a typical ductile fracture mode*

A fractography of the torn crack is shown in Fig. 14. The crack seems to penetrate into the plate limited by borders roughly perpendicular to the surface. SEM finds crack propagation edges (white lines) within the cracks revealed in the fractured surface. They are found to converge close to the bottom side of the plate. Reconstructing the origin of the crack from those white lines, it seems to be 0.2- 0.3 mm beneath the surface of the plate, but may have started along a line of 0.3 mm width parallel to the surface. They are situated approximately outside the black tinted region, which limits the propagation towards the weld seam. Hardness measurements along the cross section of weld and HAZ have revealed that this region has the highest hardness (points 3 and 14 in Fig 13). Cracks are found to initiate and propagate trans-granular through the material (Fig. 14a). In contrast, the fracture area outside the crack's region demonstrates dimples, characterizing ductile fracture (Fig. 14b).

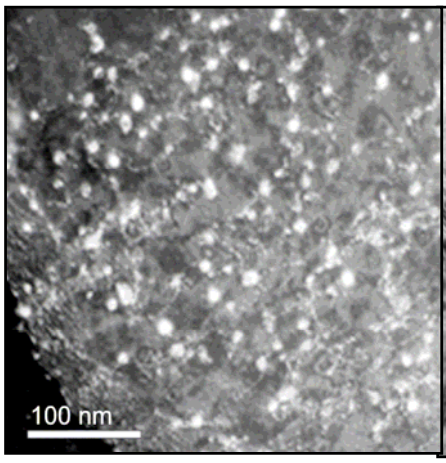

Figure 15 *TEM dark field image, showing high density of precipitation in the black tinted region*

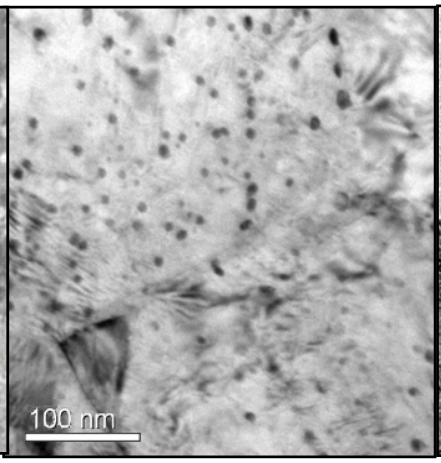

Figure 16 *TEM bright field image of precipitates in the black tinted region*

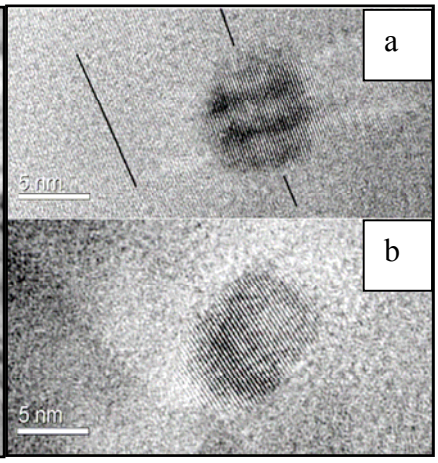

Figure 17 *HRTEM, lattice fringe contrast a) with partial coherency b) indicating non coherency of small precipitate*

The TEM investigation in Fig. 15-17 near the black-tinted region shows a very fine and high density of spherical Cu precipitates of the size < 20 nm. The HRTEM images in Fig. 17 show one set of crystallographic {111} planes within the very small precipitates with and without coherency with the matrix. According to literature [5], Cu precipitates, besides improving hardness, also traps more hydrogen and causes hydrogen diffusivity to decrease, this trapped hydrogen in the interface between Cu precipitates and matrix caused brittle fracture or cracks in HAZ. The uptake (by diffusivity and solubility) of hydrogen is influenced by microstructure and chemical composition [1]. The microstructure showing highest hardness and strength levels are most prone to hydrogen embrittlement [5 &9]. The driving force of hydrogen uptake in the alloy not only depends upon microstructure and chemical composition but also on stress gradient. Hydrogen ions tend to diffuse into the tensile stressed locations.

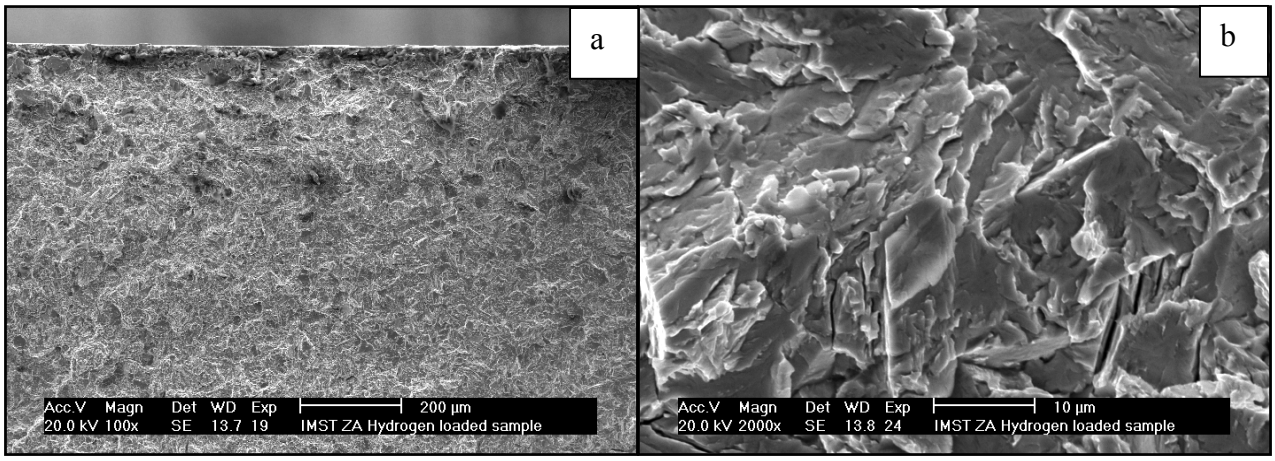

Figure 18 *a) Crack Fractography, crack was produced during hydrogen loading experiment. b) At higher magnification the crack tip is found to propagate transgrannularly in a brittle fashion*

The presence of highest hardness regions in HAZ along with the presence of residual stresses in the weld seam makes this region more susceptible structure for hydrogen embrittlement. This resulted in the form of cracks in HAZ of the welded sheet. After initiation, these cracks traveled perpendicular to the weld seam and into the plate. The black tinted region near the weld zone limited their propagation towards the fusion zone, but they continued to grow towards base metal side, where the microstructure was lath martensite with very high dislocation density. From dye penetration tests, it was found that these cracks were not produced uniformly from both sides, instead they developed from one side and some of them were big enough to pass thought the whole thickness of plate and appeared on the other side after breaking the surface. This happened due to two pass welding procedure, as the second weld pass has caused tempering and stress relieving of the fusion zone and HAZ of the first pass, hence making the second weld side more prone to hydrogen cracking, and reducing the chances of hydrogen cracking for the side which received first weld pass. Fractographic results also confirmed that these cracks originated from the second weld pass side.
Big cracks were found in the middle of the specimens submitted to the hydrogen loading, originating from the surface facing tension stress and propagated towards the other side. Fractography of these cracks (Fig. 18 a & b) show the same fracture surface as observed in HAZ. Hydrogen cracking under pre-stressed conditions in hydrogen containing environments confirmed the susceptibility of this material to hydrogen cracking.

CONCLUSIONS

The hydrogen embrittlement in the HAZ of solution treated and welded sheet of precipitation hardening stainless steel has been investigated. The optical micrographs are usually not enough to reveal the details and to characterize the microstructure of the martensite and the HAZ.
The HAZ consists of three distinct microstructural zones: retransformed martensite (and reformed austenite) with Cu in solid solution, followed by a region with Cu precipitates in the sequence overaged, peak aged and underaged. Cu precipitates increase the local hardness in the HAZ.

Cracks seem to initiate near the peak hardness region below the surface of the plate. After crack initiation, cracks propagate perpendicular to weld seem in the direction of the

under aged region in to the base metal and is limited by the overaged region. Initiation and propagation of cracks occur trans-granularly through the material.
HAZ is more prone to hydrogen embrittlement due to the presence of residual stresses produced as a result of welding and susceptible microstructure containing high density of Cu precipitates which acts as hydrogen trap sites and residual stresses provide means and directions for hydrogen transport with in the material.

It can be deduced that rapid heating and cooling cycles of welding and associated phase transformation of austenite to martensite (during cooling) and localized Cu precipitation in HAZ influenced the hydrogen uptake in HAZ and caused crack formation.

Acknowledgement:

The work was partially supported by the Austrian FFG. The authors thank Higher Education Commission of Pakistan (HEC) for sponsoring PhD studies.

References

[1] MURAYAMA, M. KATAYAMA, Y. and HONO, K. *Met. Trans.* A, Volume 30A, (1999), 345-353

[2] JUI-HUNG AND CHIH-KUANG LIN. *Met. Trans*. A, Volume 33A, June (2002), 1715-1724

[3] HSIAO, C.N., CHIOU, C.S.,.YANG, J.R *Mat. Chem. and Phys*. 74 (2002) 134-142

[4] KUMAR, A. and VENKADESAN, S. *Steel research*. 60, (1989), No. 11, 509-513

[5] CHIANG, W.,C., PU, C.,C., YU, B.,L., WU, J.,K. *Materials letters*. 57 (2003) 2485-2488

[6] WECK, E., LEISTNER, E. *Metallographische Anleitung zum Farbätzen nach dem Tauchverfahren-Teil II: Farbätzen nach Beraha und ihre Abwandlungen*. (DVS), Düsseldorf, 1982.

[7] BALA, P., SRINIVASAN, SHARKAWY, S.W., DIETZEL. W. *Mat. Sci.* & Eng. A 385 (2004) 6-12.

[8] BANERJEE, K. and CHATTERJEE U.K. *Metallurgical and materials transactions.* A, Volume 34 A, June (2003) 1297-1309

[9] TSAY, L.,W., CHI, M,.Y., WU, Y.,F., WU, J.,K., LIN., D.,Y. *Corr. Sci.* 48, (2006)1926-1938.